

Real Time Implementation of the BESS to Smoothen the output power fluctuation of the Variable Speed Wind Turbine Generator

Adnan Sattar¹, Ahmed Al Durra¹, Cedric Caruana¹, S.M Muyeen¹, Junji Tamura²

¹ Department of Electrical Engineering, The Petroleum Institute, Abu Dhabi, UAE

² Department of Electrical Engineering, Kitami Institute of Technology, Kitami, Japan

E-mail: asattar@pi.ac.ae

Abstract-- In this paper, a grid connected variable speed wind turbine (VSWT) PMSG integrated with the NaS type battery energy storage system (BESS) is modeled in the Real Time Digital Simulator (RTDS) to analyze the performance in the real system. This work is also a part of the future power hardware-in-loop (PHIL) test; therefore, individual components are modeled considering the practical viewpoints. Wind turbine, power grid and control system are modeled in the large time-step main network, however, wind generator (PMSG), frequency converter (FC), BESS integrated with STATCOM are modeled in the RTDS VSC small time-step network to adopt with the higher switching frequencies. Interface transformer is used to connect the different time-step sub network. Option of integrating the anemometer is kept open for future PHIL test. Simulation results are compared with the laboratory standard power system software PSCAD/EMTDC to validate the model developed in the RTDS/RSCAD.

Index Terms— RTDS/RSCAD, PSCAD/EMTDC, PMSG, ESS, NaS, STATCOM. Frequency Converters.

I. INTRODUCTION

Renewable energy sources often produce power and voltage varying with natural conditions (wind speed, sun light, etc). However, electric utility grid systems cannot readily accept connection of new generation plant without strict conditions placed on voltage regulation due to real power fluctuation and reactive power generation or absorption, and on voltage waveform distortion resulting from harmonic currents injected by nonlinear elements of the plant [1]. Fluctuating wind speed also causes the system frequency to deviate from the 50 Hz standard, as many protection relays have the frequency margin of 1 %, which causes the malfunction of the power system protection equipment [2]. As a result, it has become the major concern for the Transmission System Operators (TSO) or the utility companies to resolve the wind power smoothing issue [3-4]. Energy Storage System (ESS) is needed to smooth the intermittent output power fluctuations of the wind farm. A lot of choices for the ESS are present nowadays in the market e.g. Pumped Hydro Energy Storage (PHES), Compressed Air Energy Storage (CAES), Flywheel, Super capacitors Energy Storage (SES), Superconducting Magnetic Energy Storage (SMES), Hydrogen Energy Storage System (HESS), Batteries Energy Storage System (BESS), etc, which are used to overcome the fluctuated wind farm output power [5].

The choice of the ESS in the electric system network depends upon the desired application. To meet the electric power quality problems, energy storage with fast response rate and ability to charged/discharged many

times is needed [6]. For the time scale of seconds-to-minutes, a suitable energy storage system is needed to have a good ramp rates, as discussed earlier, flywheel, super capacitors, batteries might be a good option [7]. Besides that, the chosen energy storage system should be able to provide rated power for longer periods. However, for the longer time scales, the charging/discharging rate becomes less important and the choice of the ESS depends upon the amount of stored energy and the power capacity [8]. Currently, the Pumped Hydro Storage System (PHSS) is the most common storage technology for longer time scales applications [9].

Different types of batteries are presented as the substantial choice for the ESSs which are Sodium Sulfur (NaS), Lithium-Ion (Li-ion), Nickel Metal, Nickel Cadmium and Lead Acid type's batteries. Among different types of batteries, Lead Acid is the most popular and oldest technology. It has low capital investment and has the vast experience of usage. Lead-acid batteries requires frequent maintenance, they have short life (often 3-5 years), risk of explosions, acid leaking and are not environment friendly. They are majorly used as backup sources nowadays [10]. Nickel Cadmium type battery appears as an alternative for the lead-acid battery. They have longer life time, less temperature dependent and high charge rates. They have a disadvantage of crystallization; it decreases the capacity of the battery when the battery is idled. Nickel metal type hybrid battery has higher energy density as compared to the lead acid and nickel cadmium, but they need a special charging control [11].

Sodium-Sulfur (NaS) type battery system has a modular structure. It is the most recent technology among other technologies of the batteries. They are manufactured by the NGK insulators Ltd. Japan and are widely used nowadays in renewable applications as the energy storage system. NaS uses the molten metal and operates at temperature above 250° C. They have very high power densities and works good for storing bulk amount of power. They have longer life time i.e. 15 years and they are relatively inexpensive [12-13].

II. MODEL SYSTEM

The model system used in this study is shown in Fig. 1, in which individual wind generators in a wind farm is connected to the grid through the machine side inverter (MSI), DC link and grid side converter (GSC). The Permanent magnet synchronous generator (PMSG) is used as wind generator, and battery energy storage system (BESS) is adopted as the ESS. BESS consist of a DC-DC buck-boost converter, DC-AC converter and a

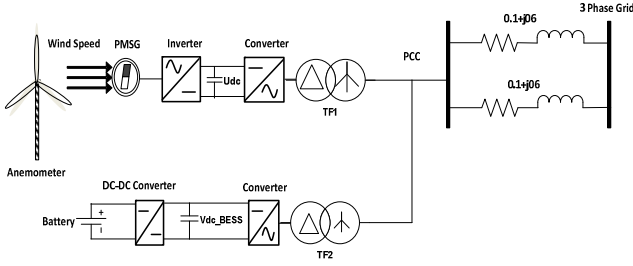


Fig. 1. Model system.

DC link capacitor, connected to the point of common coupling (PCC). Anemometer is considered to measure the wind speed signals from the real world. The wind speed is stored in the file and used in the wind turbine model of the RSCAD by using the scheduler to generate the torque for the wind generator. Hence this is the most accurate way of analyzing the behavior of the wind energy conversion system at different weather conditions.

III. REAL TIME MODELING OF THE BATTERY ENERGY STORAGE SYSTEM

The BESS has non-linear characteristics therefore the proper representation of BESS and its controllers is challenge. The simplest and most commonly used model of a battery consists of the constant internal resistance in series with the variable DC voltage source [14-15]. The battery is modeled for the amount of discharge power for an hour and the charging/discharging is limited to the 30% to 70% for the proper representation of the battery. The 5% voltage drop across the internal electromotive force of the battery is also considered, thus output of the battery voltage is $0.95 \cdot V_0$ [16]. Therefore, the total amount of energy for a 2 MW battery and discharge rate for an hour can be calculated by the following equation, $2 [MW] * 3600 [sec] = 7200 [MJ]$ (1)

The characteristics adopted for the modeling of the NaS batteries is an ideal residual capacity, its internal resistance is constant, therefore the internal electromotive force (V), discharge energy (E) can be expressed by the following equation,

$$V = -\frac{E}{7200} V_0 + V_0 \quad (2)$$

Where $E = 3600 [MJ]$, therefore the above equation will become $V = 0.95V_0$. The internal force of the NaS battery at 65% remaining capacity of NaS ($0.95V_0$) is assumed to be equal to the average of the current, I thus assumed $V_0 = 0.4971263 (kV)$ and determined. In addition, simulation, make it easier to observe the discharge of the battery charging NaS, and the remaining 65% taking the initial value of the capacitance between the upper and lower bounds. Considering the above modeling, the Fig. 2 shows the graph for the upper and lower limit of the charge/discharge of the battery.

The internal resistance for the 2 MW battery can be calculated by using the equation 3, keeping in mind the internal force and the 5% voltage drop across the resistance,

$$P_{nas} = (0.95V_0 - IR_{nas}) * I \quad (3)$$

where P_{nas} is the total capacity of the battery 2 MW, R_{nas} is the internal resistance of the battery and $0.95 V_0$ is the internal electromotive force [$V_0 = 4971263 kV$] which is assumed as mentioned earlier. Thus the

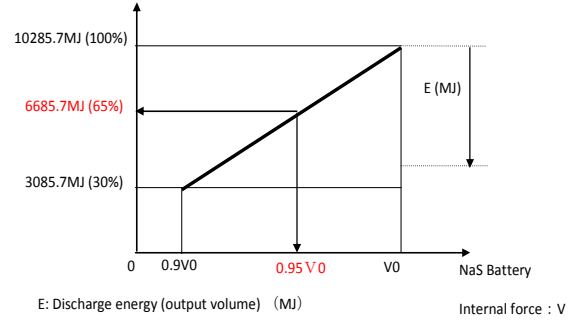


Fig. 2. Graph of the capacity of the battery, E and the internal electromotive force, V.

resistance of the battery calculated by the equation 3 is, $R_{nas} = 0.00529718 [ohm]$

The BESS is connected with the buck boost DC-DC power converter and thus appropriate control strategy is adopted for the smooth operation of the charging/discharging of BESS.

IV. BESS INTEGRATED WITH STATCOM

STATCOM is identified as the fast-responding VAR compensating device, as it suited well for the improvement of the power quality and stability problems of the wind farm. Previous studies of the STATCOM are limited only up to the reactive power compensation [15], but with the recent advancement of the BESS, it is possible to control the real power as well using BESS integrated with STATCOM system on the DC side. Thus allows us the controlling of the real and reactive power independently. Studies [17] shows that the BESS integrated with STATCOM could solved the power fluctuation problems besides that it also improves the stability of the wind farms during the short circuit disturbances by supplying the adequate reactive power support to the system. Besides that, it also has other possible applications, e.g. voltage control, frequency regulation, and power oscillation damping [18].

A. BESS control Strategy

The main objective of this control scheme is to intermittent the output power fluctuations of the VSWT generator. Therefore, a simple control strategy is taken into consideration for the control of the buck-boost DC-DC Converter. The control block diagram of the buck boost converter is shown in Fig. 3. It operates by controlling the switches of the buck boost converter by ON and OFF operation. When the power flowing to the grid, P_{grid} , is less than the desired set reference power, P_{ref} , the battery discharges and thus worked in boost converter operation mode and when the power flowing to the grid is more than the P_{ref} , then the battery will charges and worked in the buck mode operation. The error signal between the P_{grid} and P_{ref} is set through the PI controller and then compared with the triangular carrier wave generator in order to generate the switching pulses for the buck boost converter switches. The frequency of the triangular wave is chosen to be 600 Hz. Besides that, the state of charge (SOC) of battery is also considered. As it is not desired to completely discharges or overcharge the battery, the SOC of the battery should be kept within the proper limits i.e. between 30%-70%.

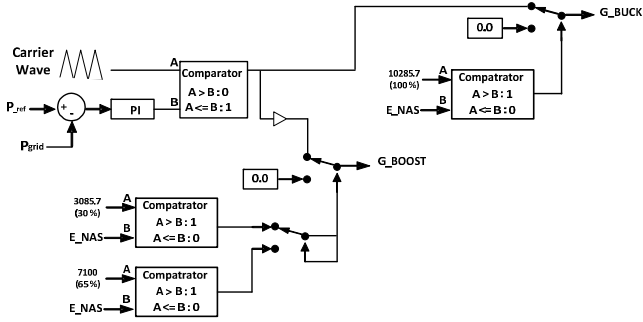


Fig. 3. Control block diagram of the BESS.

B. STATCOM control Strategy

Fig. 4 shows the control block diagram of the 2 level VSC based STATCOM. The main objective of the control of STATCOM is to provide the rapid reactive power support and keep the terminal voltage constant at its rated value. By combining the BESS with STATCOM, it offer the control of the active power, as discussed earlier. The well known cascaded vector control scheme is developed. The three phase electrical and dq quantities are related with each other by the reference frame transformation. The transformation angle is calculated by the phase locked loop (PLL) by measuring the three phase voltage signals at the PCC.

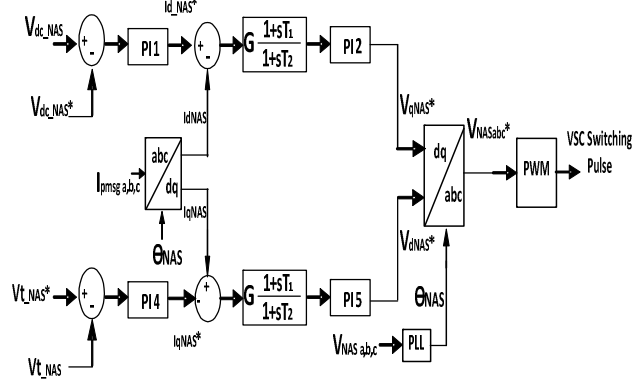


Fig. 4. Control block diagram of VSC based STATCOM.

C. PMSG and Frequency Converters

In this study, direct driven PMSG is connected to the grid through fully controlled frequency converters (FC). The FC is composed of 2-level voltage source converter, called machine side inverter (MSI) and grid side converter (GSC), are connected back-to-back.

The MSI is connected with the stator of the PMSG which efficiently decouples the PMSG to the grid, thus allowing the rotor of the wind turbine and generator to rotate freely depending on the wind speed conditions. Fig. 5 shows the control block of the MSI. Cascaded vector control scheme is used to control the real and reactive power of the PMSG generator. Park transformation is used for the reference frame transformation. The transformation angle θ_r is calculated by integrating the rotor speed of the generator. The real power reference is set in such a way to extract the maximum power from the wind energy. The reference of

the reactive power is set to zero for unity power factor operation.

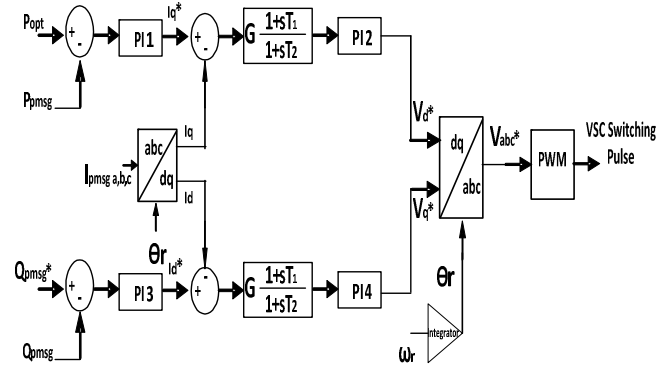


Fig. 5. Block diagram of the Machine Side Inverter.

Fig. 6 shows the control block diagram of the GSC. The main objective of the control system is to keep the DC link voltage constant and thus ensuring that active power generated by the PMSG is feed into the grid. Secondly, to control the terminal voltage through the reactive power fed or absorb from the grid. The GSC is controlled in the synchronous reference frame. The transformation angle is calculated from the three phase voltages at the high voltage side of the transformer connected at the grid side by using the PLL.

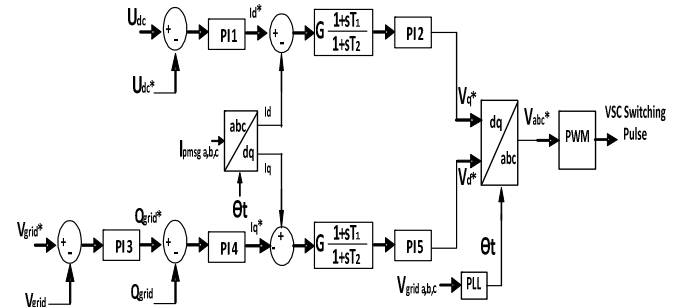


Fig. 6. Block diagram of the Grid Side Converter.

V. SWITCHING SCHEME IN THE RTDS

A Pulse width modulation (PWM) scheme is used to generate the switching pulses for the frequency converters and STATCOM. RTDS large time-step is used to generate the carrier and modulation signals. These signals are then transferred to the VSC small time-step network to generate the triangular wave by using the triangular wave generator module. VSC small time-step firing pulse generator module is used to generate the high resolution firing pulses in the small time-step environment by comparing the carrier wave and reference voltage signals. The GTO valves can get the firing pulse by selecting the option CC_WORD of the GTO Bridge [19].

VI. REAL TIME SIMULATION SETUP

In this study, the VSWT-PMSG along with the back to back inverters and the BESS integrated with the STATCOM are modeled in the small time-step of the RSCAD in order to adopt with the higher switching frequencies. The control models are developed in the

large time-step of the RSCAD. Two VSC small time-step blocks are used; one consists of the model of the VSWT-PMSG including the MSI, DC Link and GSC and the other uses the BESS integrated with the STATCOM. The two VSC small time-step blocks are solved on the different processors of the GPC cards, the different time-steps modeled are interfaced each other through the interface transformers. Wind turbine, transmission line and power grid are modeled in the RTDS large time-step and are solved on the 3PC card. The control blocks are modeled in the large time-step and are solved on the GPC card; switching signals for the switches are generated in the small time-step. The processor assignments used to solve the power network in RTDS are shown in Fig. 7.

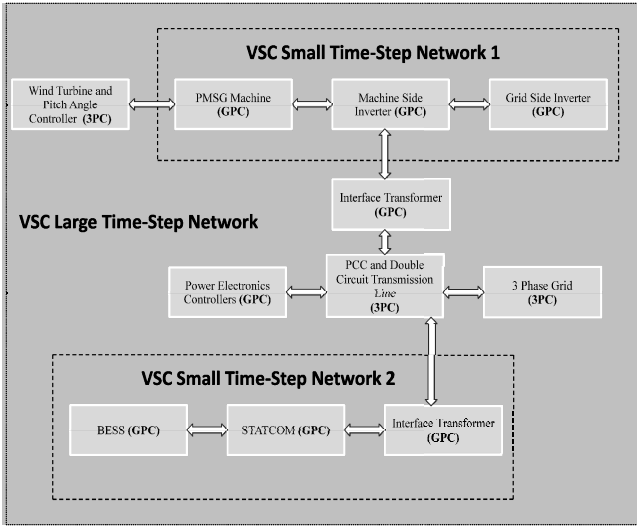


Fig. 7. Block diagram of the Modules and Processor assignments of the VSWT-PMSG and BESS integrated with STATCOM.

VII. SIMULATION RESULTS

In this paper dynamic characteristic is analyzed when the NaS type Battery Energy Storage System (BESS) integrated with the STATCOM is considered to be connected at wind farm terminal to smoothen the output power fluctuations. Real wind speed data is measured, stored in data file, and used in RTDS environment using scheduler which will finally be replaced with advanced anemometer equipped with remote data logger. Simulation results for the 300 seconds of wind speed data are shown. Switching frequency for the frequency converters, DC-DC converter and STATCOM are chosen to be 1050 Hz, 600 Hz and 1000 Hz respectively. RTDS small time-step for the VSC network 1 and 2 is 2.4 μ sec and 2.14 μ sec respectively and large time-step is chosen to be 50 μ sec. RTDS simulation results are also compared with the PSCAD/EMTDC where time-step is chosen to be 20 μ sec. The PI controller parameters are obtained by the trial and error method to obtain the finest performance.

A. RTDS/RSCAD Simulation Results

Wind speed data shown in Fig. 8 is used in the wind turbine to generate the torque for the PMSG for 300 seconds. Fig. 9 shows the RTDS responses of the VSWT-PMSG output and smoothen power to the utility grid along with the reference power signal. Fig. 10 shows the

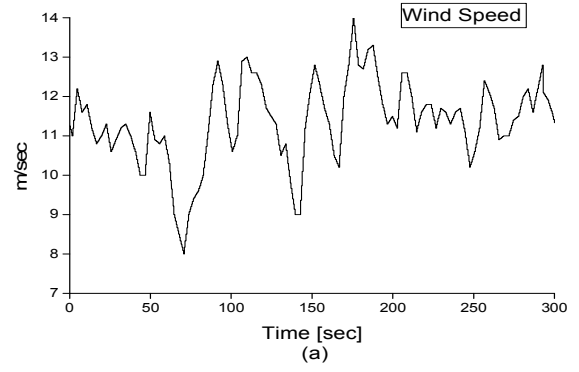


Fig. 8. Real time wind speed data.

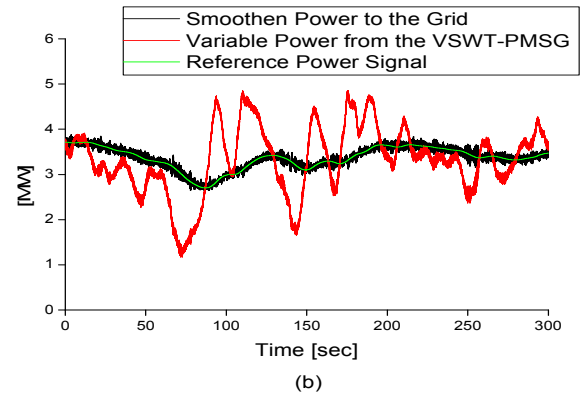


Fig. 9. RTDS responses of wind farm output and supplied power to the grid and reference power signal.

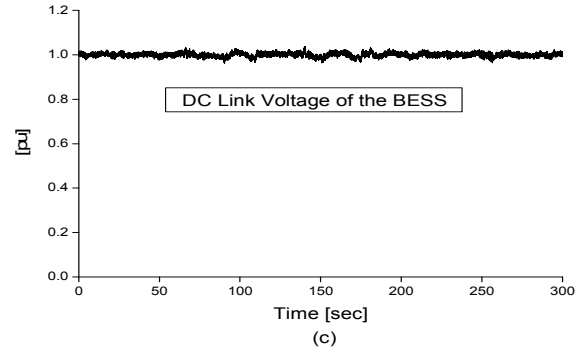


Fig. 10. RTDS response of DC Link bus voltage of the BESS.

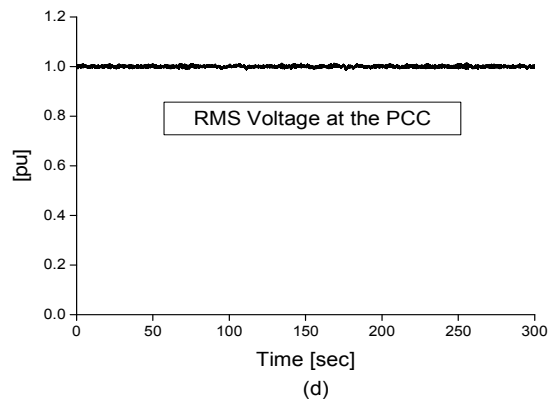


Fig. 11. RTDS response of RMS voltage at PCC.

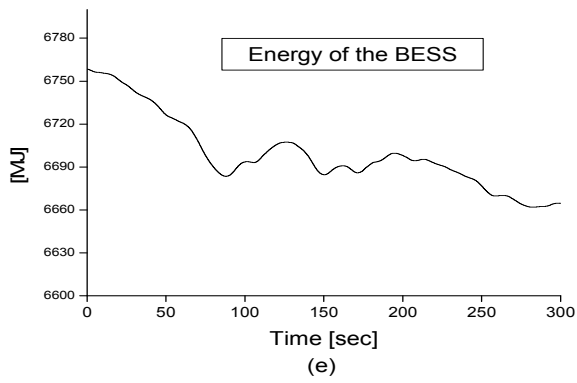


Fig. 12. RTDS response of energy level of the BESS.

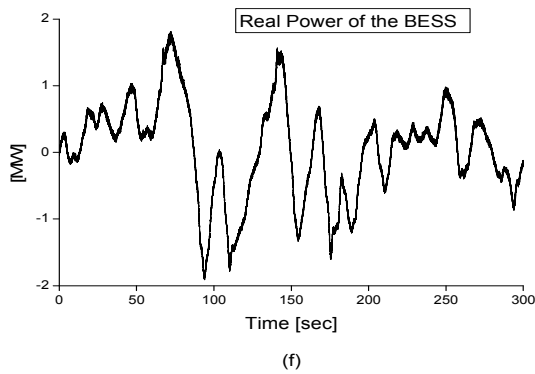


Fig. 13. RTDS response of real power supplied/absorb of the BESS.

response of the DC link bus voltage of the BESS and response of the terminal voltage at the point of common coupling (PCC) is shown in Fig. 11. The energy level of BESS that is dissipated and absorbed during the operation and real power of the battery are shown in Fig. 12 and 13 respectively. Though the DC link voltage is fluctuating as the wind farm output is fluctuating rapidly and switching operation of buck-boost converter, it is kept within $\pm 5\%$ of the rated value. The RMS voltage at PCC is kept within the rated value.

B. PSCAD/EMTDC Simulation Results

Fig. 14 till 18 shows the PSCAD/EMTDC simulation results of the smoothen power supplied to the grid, DC link bus voltage of BESS, RMS voltage at PCC, energy of the BESS and real power supplied/absorb by the

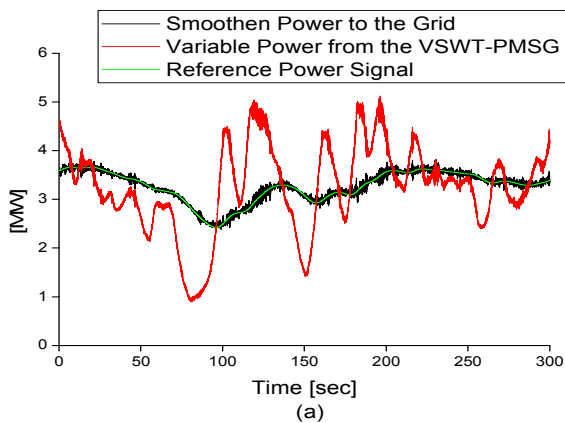


Fig. 14. PSCAD/EMTDC responses of wind farm output and supplied power to the grid and reference power signal.

BESS. The results shows good agreement with the RSCAD results, but we the variation in the RMS voltage, DC link bus voltage, power supplied to the grid are different with the RTDS results, this is because as the RSCAD uses small time-step for the simulation, the switching in the power electronic switches are very much accurate and close to the real time operation.

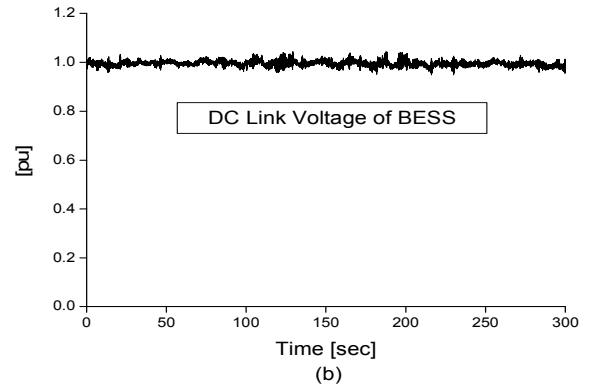


Fig. 15. PSCAD/EMTDC response of DC Link bus voltage of the BESS.

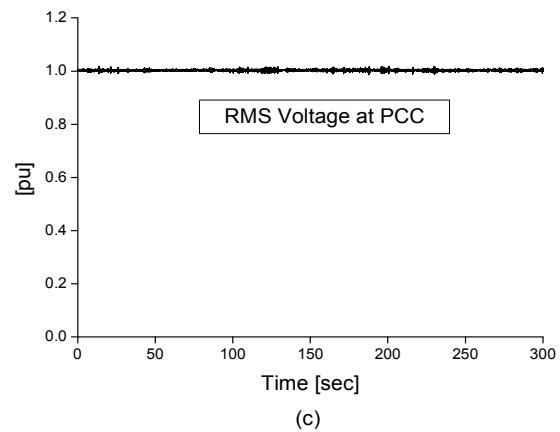


Fig. 16. PSCAD/EMTDC responses of RMS voltage at PCC.

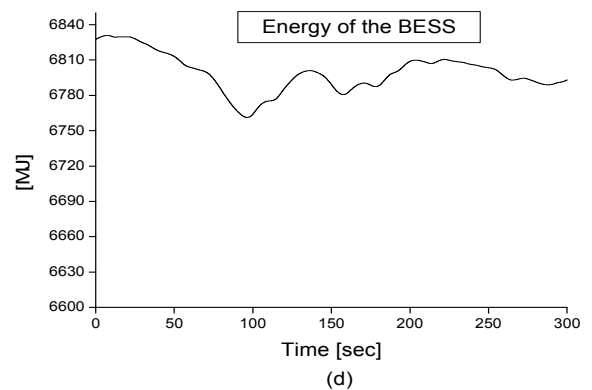


Fig. 17. PSCAD/EMTDC response of energy level of the BESS.

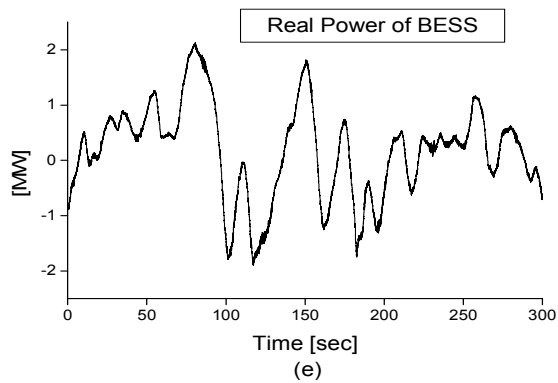


Fig. 18. PSCAD/EMTDC response of real power supplied/absorb of the BESS.

A time comparison is carried out while analyzing dynamic characteristics using 300 seconds of real wind speed data using both PSCAD/EMTDC and RTDS/RSCAD. RTDS required almost the same time of about 310seconds to download and plot the result as the simulation is running in real time with the very small time-step. However, PSCAD/EMTDC took almost 320 minutes to finish the simulation of 300sec. Therefore, it is quite difficult to perform dynamic analysis including power smoothing, optimum capacity determination for BESS, etc., for longer time in the range of hour or day using offline simulation tools. Hence, RTDS is an effective means to solve these problems.

VIII. CONCLUSION

In this study, detail modeling of the grid connected VSWT-PMSG and the NaS type BESS integrated with STATCOM is carried out in the VSC small time-step of the RTDS. Simulation results show the effectiveness of the control algorithms developed for controlling the BESS. RTDS simulation results are compared with the laboratory standard offline simulation tool i.e. PSCAD/EMTDC. VSC small time-step approach is the most precise method for studying the power system dynamics and power converters operating at higher switching frequencies. For the dynamic characteristics analysis, RTDS is proven as an effective tool due to its high computation capabilities, while the offline simulation tools are accurate but they makes simulation time longer, which is not suitable for the dynamic analysis in the range of hours or day.

RTDS hardware is expensive; therefore its processing cards should be utilized in optimum way by utilizing the 3PC processor cards when the GPC processor card is completely utilized in small time-step calculation or network calculations.

IX. REFERENCES

- [1] E.On Netz, Grid Code, High- and Extra-High Voltage, April 2006, available at www.eon-netz.com/
- [2] C. Luo and B. T. Ooi, "Frequency deviation of thermal power plants due to wind farms," *IEEE Trans. Energy Convers.*, vol. 21, no. 3, pp. 708–716, Sep. 2006.
- [3] European Network of Transmission System Operators, 2nd October 2010.

- [4] System operator market service provider, Electricity Authority – New Zeland, 11th October, 2011.
- [5] F. V. hulle, Large Scale Integration of Wind Energy in the European Power Supply Analysis, Issue and Recommendations. EWEA, Dec. 2005, Tech. Rep.
- [6] K. Divya and J. Ostergaard "Battery energy storage technology for power systems", *Electr. Power Syst. Res.*, vol. 79, no. 4, pp.511 -520 2009
- [7] H. Ibrahim, A. Ilinca, J. Perron, "Energy storage systems—characteristics and comparisons", *Renewable and Sustainable Energy Reviews*, 12 (2007), pp. 1221–1250
- [8] J. P. Barton and D. G. Infield "Energy storage and its use with intermittent renewable energy", *IEEE Trans. Energy Convers.*, vol. 19, pp.441 2004
- [9] C. Bueno, J.A. Carta, "Wind powered pumped hydro storage systems, a means of increasing the penetration of renewable energy in the Canary Islands", *Renewable and Sustainable Energy Reviews*, 10 (2006), pp. 312–340
- [10] C.J. Rydh "Environmental assessment of vanadium redox and lead-acid batteries for stationary energy storage", *J. Power Sources*, 80 (1999), pp. 21–29
- [11] Battery Power, Products and Technology, "World's Largest Battery Energy Storage System Completes Third Year of Operation", January/February 2007, Volume 11, Issue 1
- [12] Beaudin M, Zareipour H, Schellenberglabe A, Rosehart W, "Energy storage for mitigating the variability of renewable electricity sources: An updated review", *Energy for Sustainable Development* 14, 2010, p. 302-314
- [13] Polgári. B, Hartmann. B, "Energy Storage Technology for Hungary – NaS Battery for Wind Farms", *IEEE 3rd International Youth Conf.*, 7-9 July 2011, pp 1 -8
- [14] S. Teleke , M. E. Baran , A. Huang , S. Bhattacharya and L. Anderson "Control strategies for battery energy storage for wind farm dispatching", *IEEE Trans. Energy Convers.*, vol. 24, pp.725 2009
- [15] A. Sattar, A. Al-Durra, and S. M. Mueeen, "Real Time Implementation of STATCOM to Analyze Transient and Dynamic Characteristics of Wind Farm", *37th International Conference on Industrial Electronics, IEEE IECON* 7-10 Nov, 2011, Melbourne, Australia
- [16] M. Kamibayashi and K. Tanaka, "Recent Sodium Sulfur Battery Applications," *Proc. IEEE PES Transmission and Distribution Conference and Exposition, USA, 2001*, Vol. 2, 28 Oct.-2 Nov. 2001, pp. 1169-1173.
- [17] M.E. Baran, S. Teleke, L. Anderson, S. Bhattacharya, A. Huang, S. Atcitty, "STATCOM with Energy Storage for Smoothing Intermittent Wind Farm Power", *IEEE/PES*, 2008.
- [18] A. Arulampalam , M. Barnes , N. Jenkins and J. B. Ekanayake "Power quality and stability improvement of a wind farm using STATCOM supported with hybrid battery energy storage", *Proc. Inst. Electr. Eng. Gen., Transmiss. Distrib.*, vol. 153, pp.701 2006.
- [19] Real Time Digital Simulator Power System and Control User Manual, RTDS Technologies, 2009.